CITED2 IS A CONSERVED REGULATOR OF DEEP HEMOCHORIAL PLACENTATION

Marija Kuna,[1,¶,*] Pramod Dhakal,[1,¶,†] Khursheed Iqbal,[1] Esteban M. Dominguez,[1] Lindsey N. Kent,[1,‡] Masanaga Muto,[1,¥] Ayelen Moreno-Irusta,[1] Keisuke Kozai,[1,§] Kaela M. Varberg,[1] Hiroaki Okae,[2] Takahiro Arima,[2] Henry M. Sucov,[3] and Michael J. Soares[1,4,5,*]

[1]Institute for Reproduction and Perinatal Research, Department of Pathology and Laboratory Medicine, University of Kansas Medical Center, Kansas City, KS

[2]Department of Informative Genetics, Environment and Genome Research Center, Tohoku University Graduate School of Medicine, Sendai 980-8575, Japan

[3]Department of Regenerative Medicine and Cell Biology and Division of Cardiology, Department of Medicine, Medical University of South Carolina, Charleston, SC

[4]Department of Obstetrics and Gynecology, University of Kansas Medical Center, Kansas City, KS

[5]Center for Perinatal Research, Children's Research Institute, Children's Mercy, Kansas City, MO

[¶]Authors made equal contributions to the manuscript

[†]Present address: Eurofins BioPharma, Columbia, MO

[‡]Present address: Center for Reproductive Health Sciences, Department of Obstetrics and Gynecology, Washington University School of Medicine, St. Louis, MO

[¥] Present address: Department of Stem Cells and Human Disease Models, Research Center for Animal Life Science, Shiga University of Medical Science, Seta, Tsukinowa-cho, Otsu, Shiga 520-2192, Japan

[§]Present address: Department of Obstetrics and Gynecology, University of Missouri-Kansas City School of Medicine, Kansas City, MO

[*]Correspondence should be addressed: mkuna@kumc.edu or msoares@kumc.edu

Running title: CITED2 and hemochorial placentation

***Key Words*: Placenta, CITED2, trophoblast cells, plasticity**

ABSTRACT

Establishment of the hemochorial placentation site requires the exodus of trophoblast cells from the placenta and their transformative actions on the uterine vasculature, which is a critical but poorly understood developmental process. CBP/p300-interacting transactivator with glutamic acid/aspartic acid-rich carboxyl terminal domain 2 (**CITED2**) is a member of the CITED protein family of co-regulators and has been shown to possess roles in embryogenesis, including placenta development. We examined the involvement of CITED2 in the rat, which exhibits deep hemochorial placentation, a feature it shares with the human. CITED2 is distinctively expressed in the junctional zone compartment of the rat placentation site and in intrauterine invasive trophoblast cells. Homozygous disruption of the rat *Cited2* locus resulted in placental and fetal growth restriction and abnormalities in heart and lung development, which are also characteristic of the CITED2 deficient mouse model. However, other features of the mouse *Cited2* null phenotype, including exencephaly, adrenal gland agenesis, and prenatal lethality were not associated with CITED2 deficiency in the rat. Trophoblast-specific lentiviral CITED2 knockdown in the rat yielded a growth arrested placental phenotype. Smaller *Cited2* null placentas were associated with a growth restricted junctional zone and coincided with a delay in intrauterine trophoblast cell invasion. Invasive trophoblast cells arise from the junctional zone. Transcriptomes of the junctional zone, the invasive trophoblast cell lineage, and differentiating trophoblast stem cells were affected by CITED2 disruption, as were placental adaptations to hypoxia and exposure to viral mimetics. Evidence for the conservation of CITED2 expression in human placental tissue and conserved actions in invasive/extravillous trophoblast cell development were demonstrated. We conclude that CITED2 is a conserved regulator of deep hemochorial placentation.

INTRODUCTION

The hemochorial placenta creates an environment essential for survival and development of the fetus[1–3]. Several essential tasks are accomplished by the placenta. Trophoblast, the parenchymal cell lineage of the placenta, specializes into cell types facilitating the flow of nutrients into the placenta and their transfer to the fetus[3,4]. Fundamental to this process is the differentiation of trophoblast cells with the capacity to enter and transform uterine tissue proximal to the developing placenta and restructure uterine vasculature[5–8]. Intrauterine trophoblast cell invasion and trophoblast cell-guided uterine transformation are highly developed in the human and the rat, unlike the mouse[9–11]. In the human, these cells are referred to as extravillous trophoblast (**EVT**) cells and the generic term, invasive trophoblast cells, is used to identify these cells in the rat. Invasive trophoblast cell progenitors arise from structures designated as the EVT cell column and the junctional zone in the human and rat, respectively[8,12]. The EVT cell column is a well-defined structure containing a stem/proliferative population of trophoblast cells (cytotrophoblast) situated at the base of the column with a linear progression of EVT progenitor cells located within the core of the column proceeding to various stages of maturing EVT cells positioned at the distal region of the column[4,8]. In contrast, the junctional zone is more complex, giving rise to endocrine cells (trophoblast giant cells and spongiotrophoblast cells), energy reservoirs (glycogen trophoblast cells), and invasive trophoblast progenitor cells[11,13,14]. Understanding cellular decision-making within the EVT cell column and junctional zone provides insights into the development of the invasive trophoblast cell lineage.

CBP/p300 interacting transactivator, with Glu/Asp-rich carboxy terminal domain, 2 (**CITED2**) is a transcriptional co-regulator possessing the capacity to modulate interactions between DNA binding proteins and histone modifying enzymes, specifically transcription factor-CREB binding protein (**CREBBP or CBP**)/EIA binding protein p300 (**EP300**) interactions[15–17]. CBP and EP300 possess histone 3 lysine 27 (**H3K27**) acetyl transferase activity[18,19] and have been implicated in trophoblast cell differentiation and their dysregulation linked to diseases of the placenta, including preeclampsia and intrauterine growth restriction[20–23]. The outcome of CITED2 actions is transcription factor specific. In some cases, CITED2 interferes with transcription factor-CBP/EP300 interactions and inhibits gene expression (e.g. hypoxia inducible factor, **HIF**)[24–26], while in other cases, CITED2 facilitates transcription factor-CBP/EP300 recruitment and activates gene expression (e.g., Activator protein 2 family, **TFAP2**)[27,28]. Both HIF and TFAP2C (also called **AP-2γ**) have essential roles in placentation[29–33]. The connections between CITED2 and these molecular targets place CITED2 at key positions in the regulatory network controlling trophoblast cell development. In fact, mutagenesis of the mouse *Cited2* locus results in placental malformation[34,35], along with a range of other embryonic defects, including prenatal lethality[24,27,36].

In this report, we explore the involvement of CITED2 in the regulation of trophoblast cell development and deep placentation using genetically manipulated rat models and trophoblast stem (**TS**) cell models. *CITED2* is expressed prominently in the junctional zone and invasive trophoblast cells of the rat placentation site. Disruption of *Cited2* results in compromised growth of the junctional zone, abnormalities in the invasive trophoblast cell lineage, dysregulation of TS cell differentiation, and abnormalities in adaptive responses to hypoxia and immune challenges.

We also describe prominent phenotypic differences between mice and rats possessing *Cited2* null mutations. Importantly, we show that CITED2 is a conserved regulator of invasive trophoblast cell lineage decisions.

RESULTS

Cited2 expression within the rat placentation site

We started our investigation of the involvement of CITED2 in deep placentation by examining *Cited2* expression in the rat. The rat placentation site is organized into three well-defined compartments (labyrinth zone, junctional zone, uterine-placental interface) that can be enriched by dissection (**Fig. 1a**). The labyrinth zone is situated at the placental-fetal interface adjacent to the junctional zone, which borders the uterine parenchyma. As gestation progresses, invasive trophoblast cells detach from the junctional zone and infiltrate the uterine parenchyma, establishing a structure we define as the uterine-placental interface, which has also been called the metrial gland[11,12]. Reverse transcription-quantitative PCR (**RT-qPCR**) measurements demonstrated abundant expression of *Cited2* transcripts in the junctional zone (**Fig. 1b**), which was far greater than any other tissue analyzed (**Fig. 1c**). Expression of *Cited2* increased in the junctional zone and uterine-placental interface as gestation progressed (**Fig. 1b and d**). Localization of *Cited2* transcripts confirmed their presence in the junctional zone and within invasive trophoblast cells of the uterine-placental interface (**Fig. 1e**). The latter was demonstrated by co-localization of *Cited2* and *Prl7b1* transcripts. *Prl7b1* is an established marker of the invasive trophoblast cell lineage of the rat and mouse[37,38]. Thus, *Cited2* is present in compartments of the placentation site critical to the derivation (junctional zone) and functioning of invasive trophoblast cells (uterine-placental interface).

In vivo analysis following Cited2 disruption

A global *Cited2* mutant rat model was generated using *CRISPR*/Cas9 mediated genome-editing. Two guide RNAs were used to generate a 1477 bp nucleotide deletion, which removed the entire coding region of *Cited2* (**Fig. 2a**). The *Cited2* mutant allele was successfully transferred through the germline. Both male and female rats heterozygous for the *Cited2* mutation were viable and fertile. The absence of CITED2 protein in the placenta of homozygous mutants confirmed the gene disruption (**Fig. 2b**). Since *Cited2* null pups were not observed at weaning from heterozygous x heterozygous breeding, we hypothesized that *Cited2* null rats died in utero, as observed for *Cited2* mutant mice[24,27,36] or soon after birth. In contrast to the mouse, *Cited2* null mutant rats survived prenatal development and instead, died postnatally, within a few h of extrauterine life (**Supplementary Fig. 1a**). This fundamental difference prompted a more detailed comparison of the effects of *Cited2* disruption in the rat versus the mouse. We obtained a well-characterized *Cited2* mutant mouse model[24]. The *Cited2* mutation was transferred to an outbred CD1 mouse genetic background following backcrossing for >10 generations. Disruption of the *Cited2* gene in the mouse results in fetal growth restriction and a range of developmental anomalies, including: i) cardiac abnormalities; ii) arrested lung development; iii) absence of adrenal glands, and iv) neural tube defects resulting in exencephaly[24,27,36,39–42] (**Supplementary Fig. 1 and 2**). Fetal rats possessing homozygous *Cited2* mutations exhibited growth restriction (**Fig. 2c**) and heart and lung abnormalities (**Supplementary Fig. 1b-c**) as previously reported for the mouse[24,27,41,42]. At embryonic day (**E**) 15.5, all *Cited2* null rat hearts examined possessed ventral septal defects and double outlet right ventricle and half showed a retroesophageal right subclavian artery[43] (**Supplementary Fig. 1b**). Connections between abnormal placentation and

fetal heart defects have been previously described[44–46]. Postnatal day 1 lung development in *Cited2* homozygous mutant rats failed to progress and was arrested at the canicular stage[47,48] (**Supplementary Fig. 1c**). Failures in heart and lung development are probable causes of death of *Cited2* nulls on the first day of extrauterine life. In contrast to the mouse, disruption of the *Cited2* gene in the rat showed no detectable adverse effects on adrenal gland or neural tube development (**Supplementary Fig. 2**). Thus, similarities and prominent differences exist in the phenotypes of rats versus mice with *Cited2* null mutations.

CITED2 deficiency leads to placental growth restriction

In the rat, global *Cited2* deficiency resulted in placental and fetal growth restriction starting at gestation day (**gd**) 14.5 and persisting through the end of gestation (**Fig. 2c**). Similar placental growth deficits were observed for the *Cited2* null mouse (**Supplementary Fig. 3**), as previously reported[34]. Both wild type and *Cited2* null rat placentas were organized into well-defined labyrinth and junctional zone compartments; however, each compartment was significantly smaller in *Cited2* null placentation sites (**Fig. 3a and b**).

Using trophoblast-specific lentiviral delivery[49] of *Cited2*-specific short hairpin RNAs (**shRNA**)[50], we determined that the effects of CITED2 on placental size and function were trophoblast-specific (**Fig. 3d and e**). *Cited2* shRNAs were transduced into trophectoderm of blastocysts. Transduced blastocysts were transferred into pseudopregnant female rats, and placental and fetal size evaluated at gd 14.5. Placental and fetal weights were significantly smaller in *Cited2* shRNA transduced trophoblast versus control shRNA transduced trophoblast (**Fig. 3e**).

The effects of CITED2 deficiency on the junctional zone could be viewed as a cell autonomous action, whereas growth defects in the labyrinth zone as a non-cell-autonomous action, potentially arising from deficits in the junctional zone or its derivatives, including invasive trophoblast cells and their actions in transforming the uterine parenchyma.

CITED2 deficiency affects gene regulatory networks in the junctional zone

We next examined the potential cell-autonomous actions of CITED2 on junctional zone development. CITED2 is a known transcriptional co-regulator[15–17], which prompted an examination of CITED2 deficiencies on the junctional zone gene regulatory network. RNA sequencing (**RNA-seq**) was performed on gd 14.5 wild type and *Cited2* null junctional zone tissues.

A total of 203 differentially regulated transcripts were identified in the RNA-seq analysis, which included the downregulation of 160 transcripts and upregulation of 43 transcripts in CITED2 deficient junctional zone tissue (**Fig. 4a, b and e; Supplementary Table 1**). Among the downregulated transcripts were transcripts known to be prominently expressed in the junctional zone (e.g., *Prl3b1, Prl3d4, Prl8a5, Prl8a7, Prl8a9, Ccl27*). Surprisingly, an assortment of known interferon-responsive transcripts was upregulated in CITED2 deficient junctional zone tissues (e.g., *Mx2, Ifi27l2b, Isg15, Oas1f, Oasl2, Ifitm3*; **Fig. 4b**).

Rat TS cells represent an excellent model for junctional zone development[51]. Consequently, we derived rat TS cells from CITED2 deficient blastocysts and compared their

behavior to wild type rat TS cells. CITED2 deficient and wild type TS cells showed similar growth characteristics but distinct transcriptome profiles, as determined by RNA-seq (**Fig. 4c, d and f; Supplementary Fig. 4; Supplementary Table 2**). A total of 1615 differentially regulated transcripts were identified in the RNA-seq analysis, which included the downregulation of 756 transcripts and upregulation of 859 transcripts in CITED2 deficient rat TS cells. Most interestingly, there was a concordance in downregulated transcript profiles observed in CITED2 deficient TS cells and the CITED2 deficient junctional zone (**Supplementary Fig. 4).** This concordance was not as evident for upregulated transcripts, including most of the interferon-responsive transcripts, indicating that their upregulation in the CITED2 deficient junctional zone could be exacerbated by the in vivo environment.

CITED2 deficiency and invasive trophoblast cell development

Trophoblast cells invade deep into the rat uterine parenchyma[52–54]. These intrauterine invasive trophoblast cells express *Cited2* (**Fig. 1e**), implicating CITED2 as a potential regulator of the development and/or function of the invasive trophoblast cell lineage. Early endovascular trophoblast cell invasion into the decidua at gd 13.5 was limited in *Cited2* nulls in comparison to wild type placentation sites; however, as gestation progressed differences in the extent of intrauterine trophoblast invasion was not evident between *Cited2* nulls and wild type placentation sites (**Fig. 5a and b**). The invasive trophoblast cell developmental delay characteristic of *Cited2* null placentation sites was evident at gd 15.5, as visualized by in situ hybridization for *Prl7b1* and *Ceacam9* (**Fig. 5c**). Prominent phenotypic differences in wild type and CITED2 deficient invasive trophoblast cells did emerge from single cell RNA-seq (**scRNA-seq**) of the gd 18.5 uterine-placental interface (**Fig. 6b-d; Supplementary Fig. 5;**

Supplementary Table 3). Disruption of CITED2 did not prevent the development of invasive trophoblast cells but altered their phenotype and their numbers (**Fig. 6b-c**). Among the differentially expressed invasive trophoblast cell transcript signatures sensitive to CITED2 was signaling by Rho GTPases (**Fig. 6d**), which is fundamental to the regulation of cell migration and invasion[55]. Transcripts encoding cell adhesion molecules (CEACAM9, NCAM1), proteins promoting cell migration (CCDC88A), ligands targeting the vasculature (VEGFA, NPPB), and interferon-responsive proteins (IFITM3, IFI27L2B, IFI27) were differentially expressed. Interestingly, *Doxl1* was downregulated in the absence of CITED2. DOXL1 is an ortholog of AOC1, which encodes a diamine oxidase responsible for the oxidation of polyamines. AOC1 is prominently expressed in EVT cells and is dysregulated in disorders such as preeclampsia[56]. The findings indicate that CITED2 regulates the invasive trophoblast cell lineage.

CITED2 and placentation site adaptations to physiological stressors

Placentation sites possess the capacity to adapt to exposure to physiological stressors[7]. Hypoxia and polyinosinic:polycytidylic acid (**polyI:C**), a viral mimic, can elicit placental responses[57,58]. Hypoxia exposure elicits a prominent increase in endovascular trophoblast cell invasion[57], whereas polyI:C can disrupt placental and fetal development[58]. CITED2 is also connected to hypoxia and adaptations to inflammation[24–26,59–63]. Therefore, we investigated responses of wild type versus CITED2 deficient placentation sites to physiological stressors.

Maternal hypoxia exposure from gd 6.5 to 13.5 was sufficient to overcome the delay in endovascular trophoblast cell invasion observed in CITED2 deficient placentation sites (**Fig. 7a-c**). Additionally, when exposed to hypoxia CITED2 deficient conceptus sites showed an

increased resorption rate compared to their wild type littermates, indicating that without CITED2 the adaptations to hypoxia are compromised (**Fig. 7d**).

CITED2 deficiency was associated with upregulated expression of interferon-responsive transcripts in the junctional zone (**Supplementary Table 1; Fig. 4 and Fig. 6**), which implied that CITED2 could be involved in regulating responses to a viral challenge. We first determined the efficacy of a polyI:C challenge. Maternal polyI:C treatment of wild type rats resulted in significant increases in inflammatory transcript expression in the spleen and uterine-placental interface (**Supplementary Fig. 6**). We then measured interferon-responsive transcripts in wild type and *Cited2* null junctional zone tissues recovered from *Cited2* heterozygous (*Cited2*$^{+/-}$) pregnant female rats mated with *Cited*$^{+/-}$ male rats and treated with either vehicle or polyI:C. CITED2 deficiency resulted in an exaggerated response of interferon-responsive transcripts (**Fig. 7f**).

Thus, CITED2 modulates junctional zone responses to physiological stressors, including hypoxia and a viral mimetic.

CITED2 and human trophoblast cell development

There is supportive information connecting CITED2 to human placenta development and establishment of the EVT cell lineage. Partners in CITED2 action such as transcription factors (HIF1 and TFAP2C) and CBP/EP300 have been implicated as regulators of human trophoblast cell biology and placental disease[20,64–69]. *CITED2* expression is also downregulated in preeclamptic placental tissue[70]. These relationships implicating CITED2 in human placenta

pathophysiology and the above experimentation demonstrating the involvement of CITED2 in rat placentation prompted an evaluation of CITED2 in human trophoblast cell development. *CITED2* was prominently expressed in all cells constituting EVT cell columns from first trimester human placentas except for the *CDH1* positive basal cytotrophoblast progenitor cell population (**Fig. 8a**). The EVT cell column is a structure homologous to the junctional zone of the rat placentation site (**Fig. 1a**). EVT cell development can be effectively modeled in human TS cells (**Fig. 8b**)[71,72]. *CITED2* expression was significantly upregulated in EVT cells when compared to human TS cells maintained in the stem state, similar to the upregulation of *HLA-G* and *MMP2* (**Fig. 8c; Supplementary Fig. 7a**). In contrast, CITED2 transcripts decline following induction of syncytiotrophoblast differentiation (**Supplementary Fig. 7a**). Expression of *CITED1*, a paralog of CITED2 with some similar actions[17], in human TS cells was very low and declined following EVT cell differentiation (**Supplementary Fig. 7b**). We next utilized shRNA mediated CITED2 silencing to investigate the potential contributions of CITED2 to the regulation of EVT cell differentiation. CITED2 disruption effectively interfered with the expression of CITED2 and the acquisition of the signature EVT cell transcript profile (e.g. *NOTUM, FSTL3, HLA-G, HTRA4*, etc; **Fig. 8d-g**).

Collectively, the data support the involvement of CITED2 in both rat and human deep placentation.

DISCUSSION

Placentation provides a means for the fetus to grow and develop in the female reproductive tract[1,2]. The structure of the mammalian placenta exhibits elements of species specificity[73–76].

However, it is also evident that there are conserved features associated with the regulation of placental development and placental function[3,12,74]. In this report, we provide data supporting a conserved role for CITED2 in the regulation of deep placentation in the rat and in the human. CITED2 regulates events influencing development of the junctional zone compartment of the rat placenta and EVT cell column of the human placenta and their cell derivatives, invasive trophoblast cells and EVT cells, respectively. Most interestingly, CITED2 also contributes to regulating the plasticity of the placenta and its responses to physiological stressors.

The mouse and rat *Cited2* null phenotypes showed elements of conservation but also unique features. Prenatal lethality, adrenal gland agenesis, and exencephaly are hallmarks of the *Cited2* null mouse[24,27,36,40], but were not observed in the *Cited2* null rat. Distinct features of mouse and rat *Cited2* null phenotypes may be attributable to species differences in the role of CITED2 in embryonic development or more specifically, species differences in roles for the transcription factors that CITED2 modulates. At this juncture, evidence is not available to determine whether CITED2 biology in the mouse or rat better reflects CITED2 biology in other species, including the human. The absence of conservation between the mouse and rat should be cautionary regarding extrapolating findings with mutant rodent models to human pathophysiology, especially without additional supportive information. In contrast, the placenta represented a conserved target for CITED2 action in the mouse, rat, and human. The prominent expression of CITED2 in the junctional zone and EVT cell column directed our attention to investigating a role for CITED2 in the biology of these placental structures and their derivatives, invasive trophoblast/EVT cells. In the mouse, CITED2 also contributes to the regulation of the junctional zone and its derivatives[34]. Based on widespread expression of beta-galactosidase

(**lacZ**) throughout the mouse placenta in a *Cited2-lacZ* knock-in mouse model[34], CITED2 function was also investigated in the labyrinth zone[35]. Cell specific trophoblast *Cited2* disruption supported a role for CITED2 in trophoblast cell-capillary patterning and transport[35]. Although a growth restricted labyrinth zone was noted in the *Cited2* null rat, the absence, or potentially low levels, of CITED2 in the labyrinth zone implied that CITED2 was acting on the labyrinth zone in a non-cell autonomous role. The actions of CITED2 in the mouse labyrinth zone may represent another example of species-specificity of CITED2 action and could be responsible for the prenatal lethality observed in the *Cited2* null mouse.

Current evidence indicates that CITED2 acts as a co-regulator, modulating the recruitment of H3K27 acetyltransferases, CBP/EP300, to specific transcription factors controlling gene transcription[17,77]. These actions can promote or inhibit CBP/EP300-transcription factor interactions and, thus, CITED2 can serve as a facilitator of gene activation or gene repression[24–28]. TFAP2C, peroxisome proliferator activating receptor gamma (**PPARG**) and HIF1 are transcription factors affected by CITED2[24–28,61,78,79] with known actions on trophoblast cell development and placentation[80–84]. The data are consistent with CITED2 promoting placental development through stimulating transcriptional activities of transcription factors, such as TFAP2C and PPARG, and dampening placental responses to physiological stressors. CITED2 may modulate placental adaptations to hypoxia through its established role in restraining HIF-mediated transcription[24,25,59]. Linkages between CITED2 and transcription factors implicated in placentation with responses to poly I:C are not evident. However, CITED2 is an established inhibitor of immune/inflammatory responses mediated by nuclear factor kappa B[60,62] and signal transducer activator of transcription 1/interferon regulatory factor 1[63], which could contribute to

placental responses to the viral mimetic, polyI:C. CITED2 should also be viewed as an access point to other CBP/EP300-transcription factor interactions not previously known to contribute to the regulation of placentation or adaptations to physiological stressors. It is also important to appreciate that CITED2 is likely not acting as an on/off switch but instead may function as a rheostat to modulate the range of actions of specific transcription factor-CBP/EP300 interactions.

CITED2 is a member of a family of transcriptional co-regulators that in mammals also includes CITED1 and CITED4[17]. CITED1 is a known regulator of placentation in the mouse.[85–87] Connections between CITED4 and placentation have not been described. Expression profiles of CITED1 and CITED2 in the mouse placenta overlap[34,35,85], as does their interaction with CBP/EP300 and transcription factors[17]. Germline disruption of either *Cited1 or Cited2* in the mouse results in abnormal placentation, with altered junctional zone morphogenesis[34,35,85]. However, their impacts on junctional zone development differ. *Cited1* null placentas showed an expansion of the junctional zone[85], whereas *Cited2* null placentas exhibited junctional zone growth restriction[34]. Thus, how CITED1 and CITED2 cooperate to promote normal junctional zone morphogenesis is yet to be determined. We also presented evidence for the involvement of CITED2 in human EVT cell development but have not observed significant CITED1 expression in human TS cells or their derivatives[71]. Thus, there may be a species difference in the utilization of CITED family members as regulators of placental development. Rodents require two CITED family members (CITED1 and CITED2) for normal placental morphogenesis, whereas trophoblast cell lineage development in the human may only involve CITED2.

CITED2 contributes to the regulation of the invasive trophoblast/EVT cell lineage in both the rat and human. The invasive trophoblast/EVT cell lineage is critical to the establishment of a healthy hemochorial placenta[3–6]. These cells have a key role in transforming the uterus into a milieu supportive of placental and fetal development[3–6]. Their position within the uterine parenchyma and ability to adapt to physiological stressors are fundamental to a successful pregnancy. Disruptions in development and/or functioning of the invasive trophoblast/EVT cell lineage lead to pregnancy-related diseases, including preeclampsia, intrauterine growth restriction, and pre-term birth[5,6,88]. CITED2 dysregulation has been linked to preeclampsia.[70] Further interrogation of the CITED2 gene regulatory network in rat and human invasive trophoblast/EVT cells will provide insights into important developmental and pathophysiologic processes affecting hemochorial placentation and pregnancy.

MATERIALS AND METHODS

Animals

Holtzman Sprague-Dawley rats were purchased from Envigo. A CITED2 deficient mouse model[24] was a gift from Dr. Yu-Chung Yang of Case Western Reserve University (Cleveland, OH). The *Cited2* mutation was moved to a CD1 mouse genetic background following >10 generations of backcrossing. Animals were maintained in a 14 h light:10 h dark cycle (lights on at 0600 h) with food and water available ad libitum. Timed pregnancies were established by cohabiting female and male rats or mice. Mating was determined by the presence of a seminal plug or sperm in the vaginal lavage for the rat and the presence of a seminal plug in the vagina for the mouse and considered gd 0.5. Pseudopregnant female rats were generated by mating with vasectomized males. Detection of seminal plugs was considered day 0.5 of pseudopregnancy.

Hypoxia exposure. Pregnant rats were placed in a ProOX P110 gas-regulated chamber (BioSpherix) to generate a hypoxic environment [10.5% (vol/vol) oxygen] from gd 6.5 to 13.5 or gd 6.5 to 18.5 as previously described[89]. Pregnant rats exposed to ambient conditions [~21% (vol/vol) oxygen] were used as controls. Animals were euthanized at the termination of the exposures and placentation sites collected.

Poly I:C exposure. Pregnant rats were intraperitoneally injected with poly I:C (10 mg/kg body weight, P1530-25MG, Sigma-Aldrich) on gd 13.5. Animals were euthanized 6 h following injection and placentation sites collected.

The University of Kansas Medical Center (**KUMC**) Animal Care and Use Committee approved all protocols involving the use of animals.

Tissue collection and analysis

Rats and mice were euthanized by CO_2 asphyxiation at designated days of gestation. The health and viability of placentation sites and fetuses were determined. Uterine segments containing placentation sites and fetuses were frozen in dry ice-cooled heptane and stored at -80ºC until used for histological analyses. Alternatively, placentation sites were dissected. Placentas, the adjacent uterine-placental interface tissue (also referred to as the metrial gland), and fetuses were isolated as previously described.[90] Placentas were weighed and dissected into placental compartments (junctional and labyrinth zones)[90] and frozen in liquid nitrogen and stored at -80ºC until used for biochemical analyses. Fetuses were assessed for viability and morphological defects, weighed, and genotyped, and sex determined by PCR.[91] Tissues from embryonic day (**E**) 15.5 rat fetuses and postnatal day 1 (**PND1**) newborns were dissected, fixed (E15.5 fetuses: 10% neutral buffered formalin solution; PND1 newborn tissues: 4%

paraformaldehyde, **PFA**, in phosphate buffered saline, pH 7.4, **PBS**) and prepared for histological/immunohistochemical analyses. Mouse E17.5 fetal tissues were fixed in 10% neutral buffered formalin solution and tissues dissected.

Paraffin-embedded human placental tissues were obtained from the Research Centre for Women's and Children's Health Biobank (Mount Sinai Hospital, Toronto). Tissues were deidentified and collected following consent and approval by the University of Toronto and the KUMC human research ethics review committees.

Generation of a *Cited2* null rat model

CRISPR/Cas9 genome editing was utilized to generate a CITED2 deficient rat according to procedures previously described[92–95]. E0.5 zygotes were microinjected with guide RNAs targeting the entire coding region of the *Cited2* locus and Cas9 (**Fig. 1a; Supplementary Table 7**). Injected embryos were transferred to pseudopregnant rats. Offspring were screened for mutations by polymerase chain reaction (**PCR**) and verified by DNA sequencing. Founder rats possessing mutations within the *Cited2* locus were backcrossed to wild type rats to confirm germline transmission.

Genotyping and fetal sex determination

Genotyping was performed using DNA extracted from tail-tip biopsies. DNA was purified with RedExtract-N-Amp tissue PCR kit (XNAT-1000RXN, Sigma-Aldrich) using directions provided by the manufacturer. For rat *Cited2* genotyping, three primers were used to distinguish between wild type and mutant *Cited2* loci. The sequences of these primers are provided in

Supplementary Table 8. For mouse genotyping, PCR was used to detect the neomycin resistance gene, which replaced Exon 1 and part of Exon 2 of the mouse *Cited2* gene[24]. Primer sequences for mouse *Cited2* genotyping are provided in **Supplementary Table 8**. Sex of rat fetuses was determined by PCR on genomic DNA for *Kdm5c* (X chromosome) and *Kdm5d* (Y chromosome), using primers detailed in **Supplementary Table 8**, as previously described[91].

Rat blastocyst-derived TS cell culture

Wild type and *Cited2* null rat TS cells were established, maintained, and differentiated using a previously described procedure[51]. Rat TS cells were maintained in Rat TS Cell Stem State Medium (RPMI-1640 culture medium (11875093, Thermo Fisher) containing 20% fetal bovine serum (**FBS**, F2442, Sigma-Aldrich), 50 μM 2-mercaptoethanol (**2ME**, M3148, Sigma-Aldrich), 1 mM sodium pyruvate (11360070, Thermo Fisher), 100 U/ml penicillin, and 100 μg/ml streptomycin (15140122, Thermo Fisher), fibroblast growth factor 4 (**FGF4**, 25 ng/ml, 100-31, PeproTech), heparin (1 μg/ml, H3149, Sigma-Aldrich), and rat embryonic fibroblast-conditioned medium (70% of the final volume)), as previously reported[51]. Differentiation was induced by the removal of FGF4, heparin, and rat embryonic fibroblast-conditioned medium, and decreasing the FBS concentration to 1%. Rat TS cells were differentiated for 12 days.

Human TS cell culture

Human TS cells were maintained and differentiated into EVT cells using a previously described procedure[71]. Cells were cultured in 100 mm tissue culture dishes coated with 5 μg/mL collagen IV (CB40233, Thermo Fisher). Complete Human TS Cell Medium was used to maintain cells in the stem state (DMEM/F12 (11320033, Thermo Fisher), 100 μM 2ME, 0.2%

(vol/vol) FBS (16141-061, Thermo Fisher), 50 U/ml penicillin, 50 µg/mL streptomycin, 0.3% bovine serum albumin (**BSA**, BP9704100, Thermo Fisher), 1% Insulin-Transferrin-Selenium-Ethanolamine (**ITS-X**, solution (vol/vol), Thermo Fisher), 1.5 µg/mL L-ascorbic acid (A8960, Sigma-Aldrich), 50 ng/mL epidermal growth factor (**EGF**, E9644, Sigma-Aldrich), 2 µM CHIR99021 (04-0004, Reprocell), 0.5 µM A83-01 (04-0014, Reprocell), 1 µM SB431542 (04-0010, Reprocell), 0.8 mM valproic acid (P4543, Sigma-Aldrich), and 5 µM Y27632 (04-0012-02, Reprocell)). To induce EVT cell differentiation, human TS cells were plated onto 6-well plates pre-coated with 1 µg/mL collagen IV at a density of 60,000 cells per well. Cells were cultured in EVT Differentiation Medium (DMEM/F12 (11320033, Thermo Fisher), 100 µM 2ME, 50 U/ml penicillin, 50 µg/mL streptomycin, 0.3% BSA, 1% ITS-X solution, 100 ng/mL of neuregulin 1 (**NRG1**, 5218SC, Cell Signaling), 7.5 µM A83-01, 2.5 µM Y27632, 4% KnockOut Serum Replacement (**KSR**, 10828028, Thermo Fisher), and 2% Matrigel® (CB-40234, Thermo Fisher)). On day 3 of EVT cell differentiation, the medium was replaced with EVT Differentiation Medium excluding NRG1 and with a reduced Matrigel® concentration of 0.5%. On culture day 6 of EVT cell differentiation, the medium was replaced with EVT Differentiation Medium excluding NRG1 and KSR, and with a Matrigel® concentration of 0.5%. Cells were analyzed on day 8 of EVT cell differentiation. To differentiate cells into syncytiotrophoblast (ST2D and ST3D), human TS cells were plated onto 6-well plates pre-coated with 2.5 µg/mL collagen IV at a density of 100,000 cells per well (ST2D) or 6 cm Petri dishes (not cell culture treated) at a density of 300,000 cells per dish (ST3D). Cells were cultured in ST2D or ST3D Differentiation Medium (DMEM/F12, 100 µM 2ME, 50 U/ml penicillin, 50 µg/mL streptomycin, 0.3% BSA, 1% ITS-X solution, 2.5 µM Y27632, 4% KSR, 2 µM forskolin (F6886, Sigma-Aldrich), and with 50 ng/ml EGF only for ST3D culture). On day 3 of

syncytiotrophoblast differentiation, the medium was replaced with fresh ST2D or ST3D differentiation medium. Cells were analyzed on day 6 of ST2D or ST3D differentiation.

shRNA constructs and production of lentiviral particles

For rat in vivo CITED2 knockdown, *Cited2* shRNAs were designed and subcloned into pLKO.1 by using *AgeI* and *EcoRI* restriction sites as previously described[50]. For human TS cell culture, two CITED2 shRNAs were designed and subcloned independently into the pLKO.1 vector at AgeI and EcoRI restriction sites. shRNA sequences used in the analyses are included in **Supplementary Table 9**. A control shRNA that does not target any known mammalian gene, pLKO.1-shSCR (plasmid 1864), was obtained from Addgene. Lentiviral packaging vectors were obtained from Addgene and included pMDLg/pRRE (plasmid 12251), pRSVRev (plasmid 12253), and pMD2.G (plasmid 12259). Lentiviral particles were produced following transient transfection of the shRNA-pLKO.1 vector and packaging plasmids into Lenti-X (632180, Takara Bio USA) cells using Attractene (301005, Qiagen) in Opti-MEM I (51985-034, Thermo Fisher). Cells were maintained in Dulbecco's Modified Eagle Medium (DMEM, 11995-065, Thermo Fisher) supplemented with 10% FBS until 24 h prior to supernatant collection, at which time the cells were cultured in Rat TS Cell Stem State Medium for rat TS cells or Complete Human TS Cell Medium for human TS cells. Supernatants were collected every 24 h for 2 d and stored frozen at −80 °C until use.

In vivo lentiviral transduction

Rat embryos were transduced with lentiviral particles as previously described[49,96,97]. Lentiviral vector titers were determined by measurement of p24 Gag antigen by an enzyme-

linked immunosorbent assay (Advanced Bioscience Laboratories). Briefly, blastocysts collected on gd 4.5 were incubated in Acid Tyrode's Solution (EMD-Millipore) to remove zonae pellucidae and incubated with concentrated lentiviral particles (750 ng of p24/mL) for 4.5 h. Transduced blastocysts were transferred to uteri of day 3.5 pseudopregnant rats for subsequent evaluation of *Cited2* knockdown and placentation site phenotypes (**Fig. 3c**).

In vitro lentiviral transduction

Human TS cells were plated at 50,000 cells per well in 6-well tissue culture-treated plates coated with 5 µg/mL collagen IV and incubated for 24 h. Just before transduction, medium was changed, and cells were incubated with 2.5 µg/mL polybrene for 30 min at 37 °C. Immediately following polybrene incubation, TS cells were transduced with 400-600 µL of lentiviral particle containing supernatant and then incubated overnight. On the next day, medium was changed, and cells allowed to recover for 24 h. Cells were passaged, incubated for 24 h to facilitate attachment, and then selected with puromycin dihydrochloride (5 µg/mL, A11138-03, Thermo Fisher) for two days. Immediately following puromycin selection, cells were collected and EVT cell differentiation initiated.

Histological and immunohistochemical analyses

Wild type and *Cited2* null fetal, postnatal, and placental tissues were utilized for histological and immunohistochemical analyses.

Rat fetal development. E15.5 fetal tissue was fixed in 10% neutral buffered formalin, washed in **PBS**, and dehydrated. Tissues were then embedded in paraffin, 4 µm serial transverse sections were prepared, mounted on slides, and stained with hematoxylin and eosin (**H&E**). Lung and

adrenal gland tissues were dissected from PND1 neonatal rats, fixed in 4% paraformaldehyde, washed in PBS, dehydrated, and embedded in paraffin. Transverse 6 µm sections were prepared and mounted on slides. Lung development was assessed following H&E staining. Adrenal gland development was determined by immunostaining with antibodies to cytochrome P450 family 11 subfamily A member 1, (**CYP11A1**, 1:200)[98] and tyrosine hydroxylase (**TH**, 1:200, AB152, EMD Millipore). Antigen-antibody complexes were detected using Alexa Fluor 568-conjugated goat anti-rabbit IgG (A11011, Thermo Fisher) and Alexa Fluor 488-conjugated goat anti mouse IgG (A32723, Thermo Fisher) secondary antibodies and counterstained with 4,6-diamidino-2-phenylindole (**DAPI**, 1:50,000, D1306, Invitrogen).

Rat placentation sites. Frozen rat placentation sites were sectioned at 10 µm, mounted on slides, fixed in 4% PFA, and treated with H_2O_2 in methanol. Sections were blocked with 10% goat serum (50062Z, Thermo Fisher). For immunohistochemical analysis, slides were stained using vimentin primary antibody overnight at 4°C (1:300, sc-6260, Santa Cruz Biotechnology), goat anti mouse biotin as a secondary antibody for 45 min at room temperature (**RT**) (1:150, B9904, Sigma-Aldrich), ExtrAvidin-Peroxidase for 30 min at RT (1:100, E2886, Sigma-Aldrich), and AEC substrate (SK-4200, Vector Laboratories) to stain the tissue. They were then imaged using Nikon SMZ1500 stereoscopic zoom microscope. For immunofluorescence analysis sections were incubated with a pan-cytokeratin antibody (1:100 or 1:150 overnight at 4°C or for 2 h at RT, F3418, Sigma-Aldrich), perforin antibodies (1:300 overnight at 4°C, TP251, Amsbio), and DAPI (1:25,000 for 10 min at RT, D1306, Invitrogen). Immunostaining was visualized using fluorescence-tagged secondary antibodies, Alexa Fluor 488-conjugated goat anti mouse IgG (A32723, Thermo Fisher), and Alexa Fluor 568-conjugated goat anti-rabbit IgG (A11011, Thermo Fisher). Slides were mounted in Fluoromount-G (0100-01, SouthernBiotech) and

imaged on Nikon 80i or 90i upright microscopes with Photometrics CoolSNAP-ES monochrome cameras (Roper).

In situ hybridization

Cited2 transcripts in rat and human placental tissues were detected by in situ hybridization using the RNAScope® 2-plex chromogenic assay or RNAscope® Multiplex Fluorescent Reagent Kit version 2 (Advanced Cell Diagnostics), according to the manufacturer's instructions. Probes were prepared to detect rat *Cited2* (461431, NM_053698.2, target region: 2-1715), rat *Ceacam9* (1166771, NM_053919.2, target region: 130-847), rat *Prl7b1* (860181, NM_153738.1, target region: 28-900), human *CITED2* (454641, NM_006079.4, target region: 217-1771), or human *CDH1* (311091, NM_004360.3, target region: 263-1255). Images were captured on Nikon 80i or 90i upright microscopes (Nikon) with Photometrics CoolSNAP-ES monochrome cameras (Roper).

Western blotting

Expression of CITED2 protein in placental tissue was determined by western blotting. Tissue lysates were prepared in radioimmunoprecipitation assay buffer (sc-24948A, Santa Cruz Biotechnology). Protein concentrations were determined using the DC protein assay (5000112, Bio-Rad). Protein samples were separated using sodium dodecyl sulfate-polyacrylamide electrophoresis and transferred to polyvinylidene fluoride membranes (10600023, GE Healthcare). Membranes were subsequently blocked with 5% BSA in Tris buffered saline with 0.1% Tween 20 (**TBST**) and probed using antibodies specific for CITED2 (1:500, AF5005, R&D Systems) and GAPDH (1:5,000, AM4300, Invitrogen). Donkey anti-sheep

immunoglobulin G-horseradish peroxidase (**IgG-HRP**, 1:5,000, sc-2473, Santa Cruz Biotechnology) and goat anti-mouse IgG-HRP (1:5,000, 7076P2, Cell Signaling Technology) were used as secondary antibodies. Immunoreactive proteins were visualized using chemiluminescence (Immobilon Crescendo, WBLUR0500, EMD-Millipore).

RT-qPCR

Total RNA was extracted by homogenizing tissues in TRIzol (15596018, Thermo Fisher), according to the manufacturer's instructions. Purified RNA (1 μg) was used for reverse transcription using the High-Capacity cDNA Reverse Transcription kit (4368814, Applied Biosystems). Complementary DNA (**cDNA**) was diluted 1:10 and subjected to qPCR using PowerSYBR Green PCR Master Mix (4367659, Thermo Fisher), primers listed in **Supplementary Table 10**, and the QuantStudio 5 Real Time PCR system (Thermo Fisher). Cycling conditions were as follows: an initial holding step (50°C for 2 min, 95°C for 10 min), followed by 40 cycles of two-step PCR (95°C for 15 s, 60°C for 1 min), and then a dissociation step (95°C for 15 s, 60°C for 1 min, and a sequential increase to 95°C for 15 s). Relative mRNA expression was calculated using the ΔΔCt method. Glyceraldehyde 3-phosphate dehydrogenase (*Gapdh*) was used as a reference RNA for rat samples and *POLR2A* was used for human samples.

RNA-seq

Tissue from junctional zone compartments of gd 14.5 wild type and *Cited2* null placentas, wild type and *Cited2* null rat TS cells, and control and *CITED2* knockdown human TS cells were collected and processed for RNA-seq analysis. RNA was extracted using TRIzol, according to

the manufacturer's instructions. cDNA libraries (n=4/genotype for tissues and n=3/genotype for cells) were prepared with Illumina TruSeq RNA sample preparation kits (RS-122-2002, Illumina). cDNA libraries were validated for RNA integrity using an Agilent 2100 Bioanalyzer (Agilent Technologies Incorporated). cDNA libraries were clustered onto a TruSeq paired-end flow cell, and sequenced (100 bp paired-end reads) using a TruSeq 200 cycle SBS kit (Illumina). Samples were run on an Illumina HiSeq2000 sequencer (tissue specimens) or Illumina NovaSeq 6000 (cells) located at the KUMC Genome Sequencing Facility and sequenced in parallel with other samples to ensure the data generated for each run were accurately calibrated during data analysis. Reads from *.fastq files were mapped to the rat reference genome (*Rattus norvegicus* reference genome Rnor_6.0) or the human reference genome (*Homo sapiens* reference genome GRCh37) using CLC Genomics Workbench 20.0.4 (Qiagen). Only reads with <2 mismatches and minimum length and a similarity fraction of 0.8 were mapped to the reference genome. The mRNA abundance was expressed in reads per kilobase of exon per million reads mapped (**RPKM**). A p-value of 0.05 was used as a cutoff for significant differential expression (wild type versus *Cited2* null). Functional patterns of transcript expression were further analyzed using Metascape[99].

scRNA-seq

Uterine-placental interface tissues were dissected from gd 18.5 placentation sites[90], minced into small pieces, and enzymatically digested into a cell suspension for scRNA-seq as previously described[93]. Samples were then processed using Chromium Single Cell RNA-seq (10X Genomics) and libraries prepared using the Chromium Single Cell 3' (10x Genomics). Library preparation and DNA sequencing using a NovaSeq 6000 sequencer (Ilumina) were performed by

the KUMC Genome Sequencing Facility. scRNA-seq data analysis was performed as previously described[93]. Briefly, the DNA sequencing data was initially processed and analyzed using the Cell Ranger pipeline. The Seurat data pipeline (version 3.1.5) was used for additional data analysis, including identification of differentially expressed genes using *FindMarkers*[100].

Statistical analysis

Statistical analyses were performed with GraphPad Prism 9 software. Statistical comparisons were evaluated using Student's *t* test or one-way analysis of variance with Tukey's post hoc test as appropriate. Statistical significance was determined as $p<0.05$.

DATA ACCESS

All raw and processed sequencing data generated in this study have been submitted to the NCBI Gene Expression Omnibus (**GEO**) under the following accession number GSE202339.

The CITED2 mutant rat model is available through the Rat Resource and Research Center (Columbia, MO).

COMPETING INTEREST STATEMENT

There is no conflict of interest that could be perceived as prejudicing the impartiality of the research reported.

ACKNOWLEDGEMENTS

We thank Dr. Yu-Chung Yang of Case Western Reserve University (Cleveland, OH) for providing the *Cited2* mutant mouse model. We also thank Stacy Oxley and Brandi Miller for administrative assistance.

AUTHOR CONTRIBUTIONS

M.K., P.D., and M.J.S. conceived and designed the research; M.K., P.D., K.I., E.M.D., L.N.K., M.M., A.M-I., K.K., K.M.V. performed experiments; H.O., T.A. provided reagents. M.K., P.D., K.I., H.M.S., and M.J.S. analyzed the data and interpreted results of experiments; M.K., P.D., and M.J.S. prepared figures and manuscript; All authors read, contributed to editing, and approved the final version of manuscript.

REFERENCES

1. Maltepe, E. & Fisher, S. J. Placenta: the forgotten organ. *Annu Rev Cell Dev Biol* **31**, 523–552 (2015).
2. Burton, G. J., Fowden, A. L. & Thornburg, K. L. Placental origins of chronic disease. *Physiol Rev* **96**, 1509–1565 (2016).
3. Soares, M. J., Varberg, K. & Iqbal, K. Hemochorial placentation: development, function, and adaptations. *Biol Reprod* (2018).
4. Knöfler, M. *et al.* Human placenta and trophoblast development: key molecular mechanisms and model systems. *Cell Mol Life Sci* **76**, 3479–3496 (2019).
5. Kaufmann, P., Black, S. & Huppertz, B. Endovascular trophoblast invasion: implications for the pathogenesis of intrauterine growth retardation and preeclampsia. *Biol Reprod* **69**, 1–7 (2003).
6. Pijnenborg, R., Vercruysse, L. & Hanssens, M. The uterine spiral arteries in human pregnancy: facts and controversies. *Placenta* **27**, 939–958 (2006).
7. Soares, M. J., Chakraborty, D., Kubota, K., Renaud, S. J. & Rumi, M. A. K. Adaptive mechanisms controlling uterine spiral artery remodeling during the establishment of pregnancy. *Int J Dev Biol* **58**, 247–259 (2014).
8. Pollheimer, J., Vondra, S., Baltayeva, J., Beristain, A. G. & Knöfler, M. Regulation of placental extravillous trophoblasts by the maternal uterine environment. *Front Immunol* **9**, 2597 (2018).
9. Pijnenborg, R., Robertson, W. B., Brosens, I. & Dixon, G. Trophoblast invasion and the establishment of haemochorial placentation in man and laboratory animals. *Placenta* **2**, 71–91 (1981).
10. Pijnenborg, R. & Vercruysse, L. Animal models of deep trophoblast invasion. In Placental bed disorders: basic science and its translation to obstetrics (eds R Pijnenborg, I Brosens, R Romero). Cambridge University Press, Cambridge, 127–139 (2010).
11. Soares, M. J., Chakraborty, D., Rumi, M. A. K., Konno, T. & Renaud, S. J. Rat placentation: An experimental model for investigating the hemochorial maternal-fetal interface. *Placenta* **33**, 233–243 (2012).
12. Varberg, K. M. & Soares, M. J. Paradigms for investigating invasive trophoblast cell development and contributions to uterine spiral artery remodeling. *Placenta* **113**, 48–56 (2021).
13. Soares, M. J. *et al.* Differentiation of trophoblast endocrine cells. *Placenta* **17**, 277–289 (1996).
14. Simmons, D. G. & Cross, J. C. Determinants of trophoblast lineage and cell subtype specification in the mouse placenta. *Dev Biol* **284**, 12–24 (2005).
15. Du, J. & Yang, Y.-C. Cited2 in hematopoietic stem cell function. *Curr Opin Hematol* **20**, 301–307 (2013).
16. An, B., Ji, X. & Gong, Y. Role of CITED2 in stem cells and cancer. *Oncol Lett* **20**, 1–1 (2020).
17. Bragança, J., Mendes-Silva, L., Lopes, J. A. & Calado, S. M. CITED proteins in the heart of pluripotent cells and in heart's full potential. *Regen Med Front* **1**, e3190005 (2019).
18. Kalkhoven, E. CBP and p300: HATs for different occasions. *Biochem Pharmacol* **68**, 1145–1155 (2004).

19. Voss, A. K. & Thomas, T. Histone lysine and genomic targets of histone acetyltransferases in mammals. *Bioessays* **40**, e1800078 (2018).
20. van Uitert, M. *et al.* Meta-analysis of placental transcriptome data identifies a novel molecular pathway related to preeclampsia. *PLoS One* **10**, e0132468 (2015).
21. Fergelot, P. *et al.* Phenotype and genotype in 52 patients with Rubinstein–Taybi syndrome caused by EP300 mutations. *Am J Med Genet A* **170**, 3069–3082 (2016).
22. Paauw, N. D. *et al.* H3K27 acetylation and gene expression analysis reveals differences in placental chromatin activity in fetal growth restriction. *Clin Epigenetics* **10**, 85 (2018).
23. Zhang, B. *et al.* Human placental cytotrophoblast epigenome dynamics over gestation and alterations in placental disease. *Dev Cell* **56**, 1238-1252.e5 (2021).
24. Yin, Z. *et al.* The essential role of Cited2, a negative regulator for HIF-1alpha, in heart development and neurulation. *Proc Natl Acad Sci USA* **99**, 10488–10493 (2002).
25. Freedman, S. J. *et al.* Structural basis for negative regulation of hypoxia-inducible factor-1alpha by CITED2. *Nat Struct Biol* **10**, 504–512 (2003).
26. Berlow, R. B., Dyson, H. J. & Wright, P. E. Hypersensitive termination of the hypoxic response by a disordered protein switch. *Nature* **543**, 447–451 (2017).
27. Bamforth, S. D. *et al.* Cardiac malformations, adrenal agenesis, neural crest defects and exencephaly in mice lacking Cited2, a new Tfap2 co-activator. *Nat Genet* **29**, 469–474 (2001).
28. Bragança, J. *et al.* Physical and functional interactions among AP-2 transcription factors, p300/CREB-binding protein, and CITED2. *J Biol Chem* **278**, 16021–16029 (2003).
29. Adelman, D. M., Gertsenstein, M., Nagy, A., Simon, M. C. & Maltepe, E. Placental cell fates are regulated in vivo by HIF-mediated hypoxia responses. *Genes Dev* **14**, 3191–3203 (2000).
30. Auman, H. J. *et al.* Transcription factor AP-2gamma is essential in the extra-embryonic lineages for early postimplantation development. *Development* **129**, 2733–2747 (2002).
31. Werling, U. & Schorle, H. Transcription factor gene AP-2gamma essential for early murine development. *Mol Cell Biol* **22**, 3149–3156 (2002).
32. Cowden Dahl, K. D. *et al.* Hypoxia-inducible factors 1alpha and 2alpha regulate trophoblast differentiation. *Mol Cell Biol* **25**, 10479–10491 (2005).
33. Sharma, N. *et al.* Tpbpa-Cre-mediated deletion of TFAP2C leads to deregulation of Cdkn1a, Akt1 and the ERK pathway, causing placental growth arrest. *Development* **143**, 787–798 (2016).
34. Withington, S. L. *et al.* Loss of Cited2 affects trophoblast formation and vascularization of the mouse placenta. *Dev Biol* **294**, 67–82 (2006).
35. Moreau, J. L. M. *et al.* Cited2 is required in trophoblasts for correct placental capillary patterning. *Dev Biol* **392**, 62–79 (2014).
36. Barbera, J. P. M. *et al.* Folic acid prevents exencephaly in Cited2 deficient mice. *Hum Mol Genet* **11**, 283–293 (2002).
37. Wiemers, D. O., Ain, R., Ohboshi, S. & Soares, M. J. Migratory trophoblast cells express a newly identified member of the prolactin gene family. *J Endocrinol* **179**, 335–346 (2003).
38. Bu, P., Alam, S. M. K., Dhakal, P., Vivian, J. L. & Soares, M. J. A prolactin family paralog regulates placental adaptations to a physiological stressor. *Biol Reprod* **94**, 107 (2016).
39. Schneider, J. E. *et al.* Rapid identification and 3D reconstruction of complex cardiac malformations in transgenic mouse embryos using fast gradient echo sequence magnetic resonance imaging. *J Mol Cell Cardiol* **35**, 217–222 (2003).

40. Schneider, J. E. *et al.* High-resolution imaging of normal anatomy, and neural and adrenal malformations in mouse embryos using magnetic resonance microscopy. *J Anat* **202**, 239–247 (2003).
41. Xu, B. *et al.* Cited2 is required for fetal lung maturation. *Dev Biol* **317**, 95–105 (2008).
42. Lopes Floro, K. *et al.* Loss of Cited2 causes congenital heart disease by perturbing left–right patterning of the body axis. *Hum Mol Genet* **20**, 1097–1110 (2011).
43. Savolainen, S. M., Foley, J. F. & Elmore, S. A. Histology atlas of the developing mouse heart with emphasis on E11.5 to E18.5. *Toxicol Pathol* **37**, 395–414 (2009).
44. Camm, E. J., Botting, K. J. & Sferruzzi-Perri, A. N. Near to One's Heart: The Intimate Relationship Between the Placenta and Fetal Heart. *Front Physiol* **9**, 629 (2018).
45. Perez-Garcia, V. *et al.* Placentation defects are highly prevalent in embryonic lethal mouse mutants. *Nature* **555**, 463–468 (2018).
46. Courtney, J. A., Cnota, J. F. & Jones, H. N. The Role of Abnormal Placentation in Congenital Heart Disease; Cause, Correlate, or Consequence? *Front Physiol* **9**, 1045 (2018).
47. Morrisey, E. E. & Hogan, B. L. M. Preparing for the first breath: genetic and cellular mechanisms in lung development. *Dev Cell* **18**, 8–23 (2010).
48. O'Reilly, M. & Thébaud, B. Animal models of bronchopulmonary dysplasia. The term rat models. *Am J Physiol Lung Cell Mol Physiol* **307**, L948–L958 (2014).
49. Lee, D.-S., Rumi, M. A. K., Konno, T. & Soares, M. J. In vivo genetic manipulation of the rat trophoblast cell lineage using lentiviral vector delivery. *Genesis* **47**, 433–439 (2009).
50. Imakawa, K. *et al.* CITED2 modulation of trophoblast cell differentiation: insights from global transcriptome analysis. *Reproduction* **151**, 509–516 (2016).
51. Asanoma, K. *et al.* FGF4-dependent stem cells derived from rat blastocysts differentiate along the trophoblast lineage. *Dev Biol* **351**, 110–119 (2011).
52. Ain, R., Canham, L. N. & Soares, M. J. Gestation stage-dependent intrauterine trophoblast cell invasion in the rat and mouse: novel endocrine phenotype and regulation. *Dev Biol* **260**, 176–190 (2003).
53. Caluwaerts, S., Vercruysse, L., Luyten, C. & Pijnenborg, R. Endovascular trophoblast invasion and associated structural changes in uterine spiral arteries of the pregnant rat. *Placenta* **26**, 574–584 (2005).
54. Vercruysse, L., Caluwaerts, S., Luyten, C. & Pijnenborg, R. Interstitial trophoblast invasion in the decidua and mesometrial triangle during the last third of pregnancy in the rat. *Placenta* **27**, 22–33 (2006).
55. Guan, X., Guan, X., Dong, C. & Jiao, Z. Rho GTPases and related signaling complexes in cell migration and invasion. *Exp Cell Res* **388**, 111824 (2020).
56. Velicky, P. *et al.* Pregnancy-associated diamine oxidase originates from extravillous trophoblasts and is decreased in early-onset preeclampsia. *Sci Rep* **8**, 6342 (2018).
57. Rosario, G. X., Konno, T. & Soares, M. J. Maternal hypoxia activates endovascular trophoblast cell invasion. *Dev Biol* **314**, 362–375 (2008).
58. Baines, K. J. *et al.* Antiviral inflammation during early pregnancy reduces placental and fetal growth trajectories. *J Immunol* **204**, 694–706 (2020).
59. Bhattacharya, S. *et al.* Functional role of p35srj, a novel p300/CBP binding protein, during transactivation by HIF-1. *Genes Dev* **13**, 64–75 (1999).
60. Lou, X. *et al.* Negative feedback regulation of NF-κB action by CITED2 in the nucleus. *J Immunol* **186**, 539–548 (2011).

61. Kim, G.-D. *et al.* CITED2 restrains pro-inflammatory macrophage activation and response. *Mol Cell Biol* **38**, e00452-17 (2018).
62. Pong Ng, H., Kim, G.-D., Ricky Chan, E., Dunwoodie, S. L. & Mahabeleshwar, G. H. CITED2 limits pathogenic inflammatory gene programs in myeloid cells. *FASEB J* **34**, 12100–12113 (2020).
63. Zafar, A. *et al.* CITED2 inhibits STAT1-IRF1 signaling and atherogenesis. *FASEB J.* **35**, e21833 (2021).
64. Wakeland, A. K. *et al.* Hypoxia directs human extravillous trophoblast differentiation in a hypoxia-inducible factor-dependent manner. *Am J Pathol* **187**, 767–780 (2017).
65. Krendl, C. *et al.* GATA2/3-TFAP2A/C transcription factor network couples human pluripotent stem cell differentiation to trophectoderm with repression of pluripotency. *Proc Natl Acad Sci USA* **114**, E9579–E9588 (2017).
66. Foley, P., Bunyan, D., Stratton, J., Dillon, M. & Lynch, S. A. Further case of Rubinstein–Taybi syndrome due to a deletion in EP300. *Am J Med Genet A* **149A**, 997–1000 (2009).
67. Tsai, A. C.-H. *et al.* Exon deletions of the EP300 and CREBBP genes in two children with Rubinstein–Taybi syndrome detected by aCGH. *Eur J Hum Genet* **19**, 43–49 (2011).
68. Solomon, B. D. *et al.* Expanding the phenotypic spectrum in EP300-related Rubinstein–Taybi syndrome. *Am J Med Genet A* **167A**, 1111–1116 (2015).
69. Wincent, J. *et al.* CREBBP and EP300 mutational spectrum and clinical presentations in a cohort of Swedish patients with Rubinstein–Taybi syndrome. *Mol Genet Genomic Med* **4**, 39–45 (2016).
70. Nishizawa, H. *et al.* Microarray analysis of differentially expressed fetal genes in placental tissue derived from early and late onset severe pre-eclampsia. *Placenta* **28**, 487–497 (2007).
71. Okae, H. *et al.* Derivation of human trophoblast stem cells. *Cell Stem Cell* **22**, 50-63.e6 (2018).
72. Shibata, S. *et al.* Unique features and emerging in vitro models of human placental development. *ReprodMed Biol* **19**, 301–313 (2020).
73. Carter, A. M. & Enders, A. C. Comparative aspects of trophoblast development and placentation. *Reprod Biol Endocrinol* **2**, 46 (2004).
74. Soncin, F., Natale, D. & Parast, M. M. Signaling pathways in mouse and human trophoblast differentiation: a comparative review. *Cell Mol Life Sci* **72**, 1291–1302 (2015).
75. Roberts, R. M., Green, J. A. & Schulz, L. C. The evolution of the placenta. *Reproduction* **152**, R179–R189 (2016).
76. Carter, A. M. Unique aspects of human placentation. *Int J Mol Sci* **22**, 8099 (2021).
77. Bhattacharya, S. & Ratcliffe, P. J. ExCITED about HIF. *Nat Struct Biol* **10**, 501–503 (2003).
78. Tien, E. S., Davis, J. W. & Vanden Heuvel, J. P. Identification of the CREB-binding protein/p300-interacting protein CITED2 as a peroxisome proliferator-activated receptor alpha coregulator. *J Biol Chem* **279**, 24053–24063 (2004).
79. Gonzalez, Y. R. *et al.* CITED2 signals through peroxisome proliferator-activated receptor-gamma to regulate death of cortical neurons after DNA damage. *J Neurosci* **28**, 5559–5569 (2008).
80. Kuckenberg, P., Kubaczka, C. & Schorle, H. The role of transcription factor Tcfap2c/TFAP2C in trophectoderm development. *Reprod Biomed Online* **25**, 12–20 (2012).
81. Fournier, T., Therond, P., Handschuh, K., Tsatsaris, V. & Evain-Brion, D. PPARgamma and early human placental development. *Curr Med Chem* **15**, 3011–3024 (2008).

82. Barak, Y., Sadovsky, Y. & Shalom-Barak, T. PPAR signaling in placental development and function. *PPAR Res* **2008**, e142082 (2007).
83. Soares, M. J., Iqbal, K. & Kozai, K. Hypoxia and placental development. *Birth Defects Res* **109**, 1309–1329 (2017).
84. Chang, C.-W., Wakeland, A. K. & Parast, M. M. Trophoblast lineage specification, differentiation and their regulation by oxygen tension. *J Endocrinol* **236**, R43–R56 (2018).
85. Rodriguez, T. A. *et al.* Cited1 is required in trophoblasts for placental development and for embryo growth and survival. *Mol Cell Biol* **24**, 228–244 (2004).
86. Sparrow, D. B. *et al.* Placental insufficiency associated with loss of Cited1 causes renal medullary dysplasia. *J Am Soc Nephrol* **20**, 777–786 (2009).
87. Xu, Y. *et al.* Transcription coactivator Cited1 acts as an inducer of trophoblast-like state from mouse embryonic stem cells through the activation of BMP signaling. *Cell Death Dis* **9**, 1–17 (2018).
88. Brosens, I., Puttemans, P. & Benagiano, G. Placental bed research: I. The placental bed: from spiral arteries remodeling to the great obstetrical syndromes. *Am J Obstet Gynecol* **221**, 437–456 (2019).
89. Chakraborty, D., Scott, R. L. & Soares, M. J. Hypoxia signaling and placental adaptations. *Methods Mol Biol* **1742**, 167–183 (2018).
90. Ain, R., Konno, T., Canham, L. N. & Soares, M. J. Phenotypic analysis of the rat placenta. *Methods Mol Med* **121**, 295–313 (2006).
91. Dhakal, P. & Soares, M. J. Single-step PCR-based genetic sex determination of rat tissues and cells. *Biotechniques* **62**, 232–233 (2017).
92. Varberg, K. M. *et al.* ASCL2 reciprocally controls key trophoblast lineage decisions during hemochorial placenta development. *Proc Natl Acad Sci USA* **118**, e2016517118 (2021).
93. Iqbal, K. *et al.* Evaluation of placentation and the role of the aryl hydrocarbon receptor pathway in a rat model of dioxin exposure. *Environ Health Perspect* **129**, 117001 (2021).
94. Iqbal, K., Dhakal, P., Pierce, S. H. & Soares, M. J. Catechol-O-methyltransferase and Pregnancy Outcome: an Appraisal in Rat. *Reprod Sci* **28**, 462–469 (2021).
95. Muto, M. *et al.* Intersection of regulatory pathways controlling hemostasis and hemochorial placentation. *Proc Natl Acad Sci USA* **118**, e2111267118 (2021).
96. Kent, L. N., Rumi, M. A. K., Kubota, K., Lee, D.-S. & Soares, M. J. FOSL1 is integral to establishing the maternal-fetal interface. *Mol Cell Biol* **31**, 4801–4813 (2011).
97. Chakraborty, D., Muto, M. & Soares, M. J. Ex vivo trophoblast-specific genetic manipulation using lentiviral delivery. *Bio Protoc* **7**, e2652 (2017).
98. Roby, K. F., Larsen, D., Deb, S. & Soares, M. J. Generation and characterization of antipeptide antibodies to rat cytochrome P-450 side-chain cleavage enzyme. *Mol Cell Endocrinol* **79**, 13–20 (1991).
99. Zhou, Y. *et al.* Metascape provides a biologist-oriented resource for the analysis of systems-level datasets. *Nat Commun* **10**, 1523 (2019).
100. Stuart, T. *et al.* Comprehensive integration of single-cell data. *Cell* **177**, 1888-1902.e21 (2019).

FIGURES

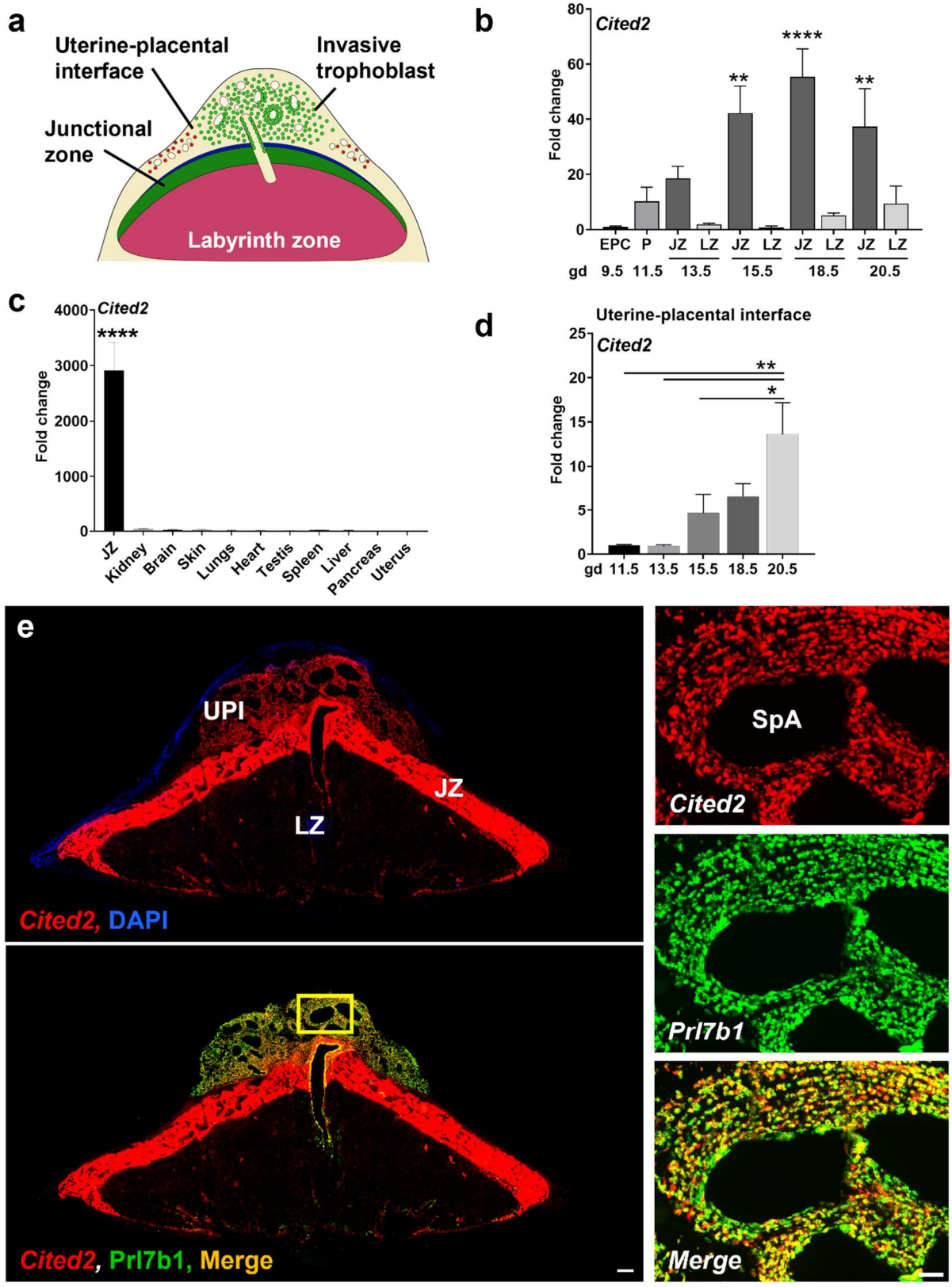

Fig. 1 *Cited2* transcript expression in the placenta and uterine-placental interface during gestation in the rat. a. Schematic showing the rat placentation site. Invaded trophoblast cells are depicted in green. **b.** Relative expression of *Cited2* transcripts in the ectoplacental cone (**EPC**), whole placenta (**P**), junctional zone (**JZ**), and labyrinth zone (**LZ**) of the rat placenta during gestation. Values depicted were normalized to EPC 9.5 samples. **c.** Relative expression of *Cited2* transcript in postnatal day 1 (**PND1**) rat neonatal tissues and gd 14.5 JZ tissue. **d.** Relative expression of *Cited2* transcripts within the uterine-placental interface during gestation. **e.** *In situ* hybridization showing *Cited2* transcript distribution (top left) and *Cited2* and *Prl7b1* (invasive trophoblast marker) transcript co-localization in rat gestation day (**gd**) 18.5 placentation site (bottom left). Higher magnification images of the area outlined by a yellow rectangle (bottom left) are shown to the right. Scale bar=500 μm (left panels), scale bar=100 μm (right panels). Uterine-placental interface (**UPI**), spiral artery (**SpA**). The histograms presented in panels b, c, and d represent means ± SEM, n=5-10, 3-6 pregnancies. One-way ANOVA, Tukey's post hoc test, * $p < 0.05$, ** $p < 0.01$, **** $p<0.0001$.

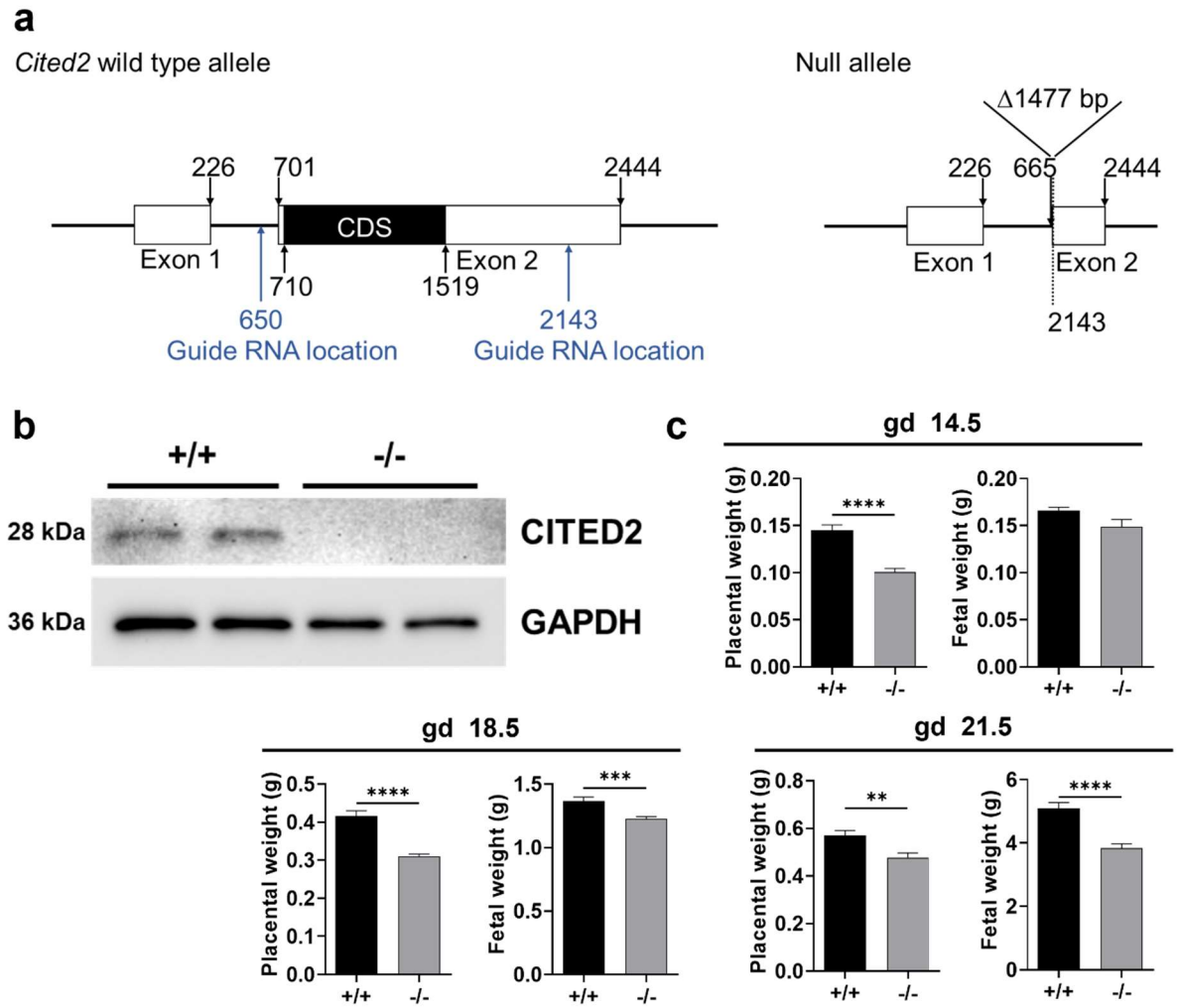

Fig. 2 Disruption of the *Cited2* locus in the rat. a. Schematic of the *Cited2* wild type and null alleles. A 1477 bp deletion was generated using *CRISPR*/Cas9 genome editing. The deletion included the entire coding sequence of the *Cited2* gene. **b.** Western blot for CITED2 protein in rat junctional zone tissue samples from *Cited2*$^{+/-}$ x *Cited2*$^{+/-}$ breeding on gd 18.5. **c.** Fetal and placental weights from *Cited2*$^{+/-}$ x *Cited2*$^{+/-}$ breeding for the rat. Values represent mean ± SEM, n=17-35, unpaired t-test, **p<0.01, ***p<0.001, **** p<0.0001.

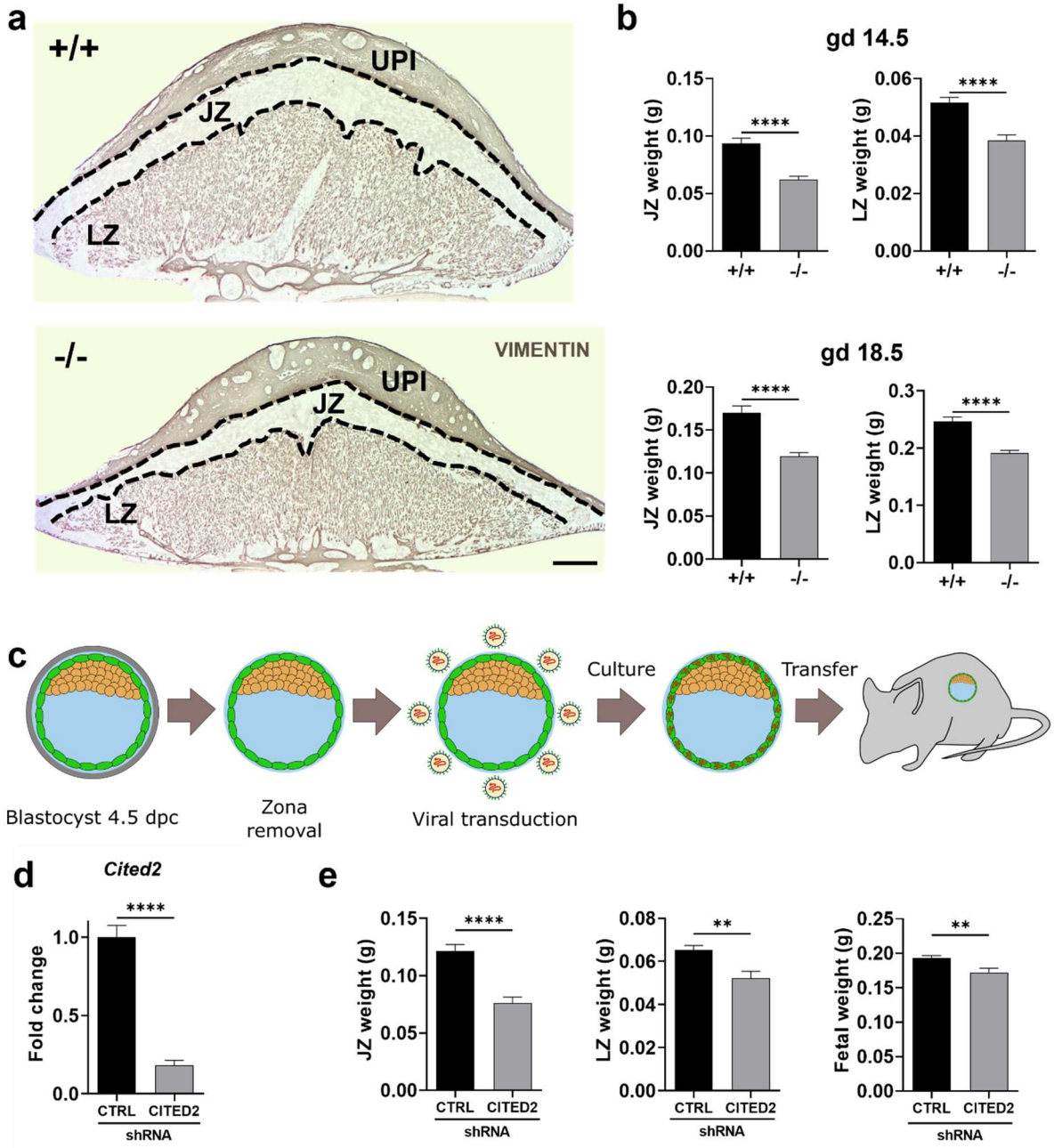

Fig. 3 The CITED2 deficient rat placenta is growth restricted. a. Immunohistological analysis of vimentin in wild type (**WT,** +/+) and null (-/-) placentas from *Cited2*$^{+/-}$ x *Cited2*$^{+/-}$ breeding on gd 18.5. Scale bar=1000 µm. UPI uterine-placental interface, JZ junctional zone, LZ labyrinth zone. **b.** JZ and LZ weights from *Cited2*$^{+/-}$ x *Cited2*$^{+/-}$ breeding on gd 14.5 and gd 18.5. **c.** Simplified schematic depicting the strategy for achieving trophoblast specific CITED2 knockdown in vivo. **d**. Relative expression of *Cited2* transcripts in control (**CTRL**) and CITED2 shRNA-exposed gd 14.5 JZ. **e.** JZ, LZ and fetal weights from control and gd 14.5 trophoblast specific *Cited2* knockdown. CTRL, control knockdown, KD, *Cited2* knockdown. Shown are mean values ± SEM, n=12-20, unpaired t-test, **p<0.01, **** p<000.1.

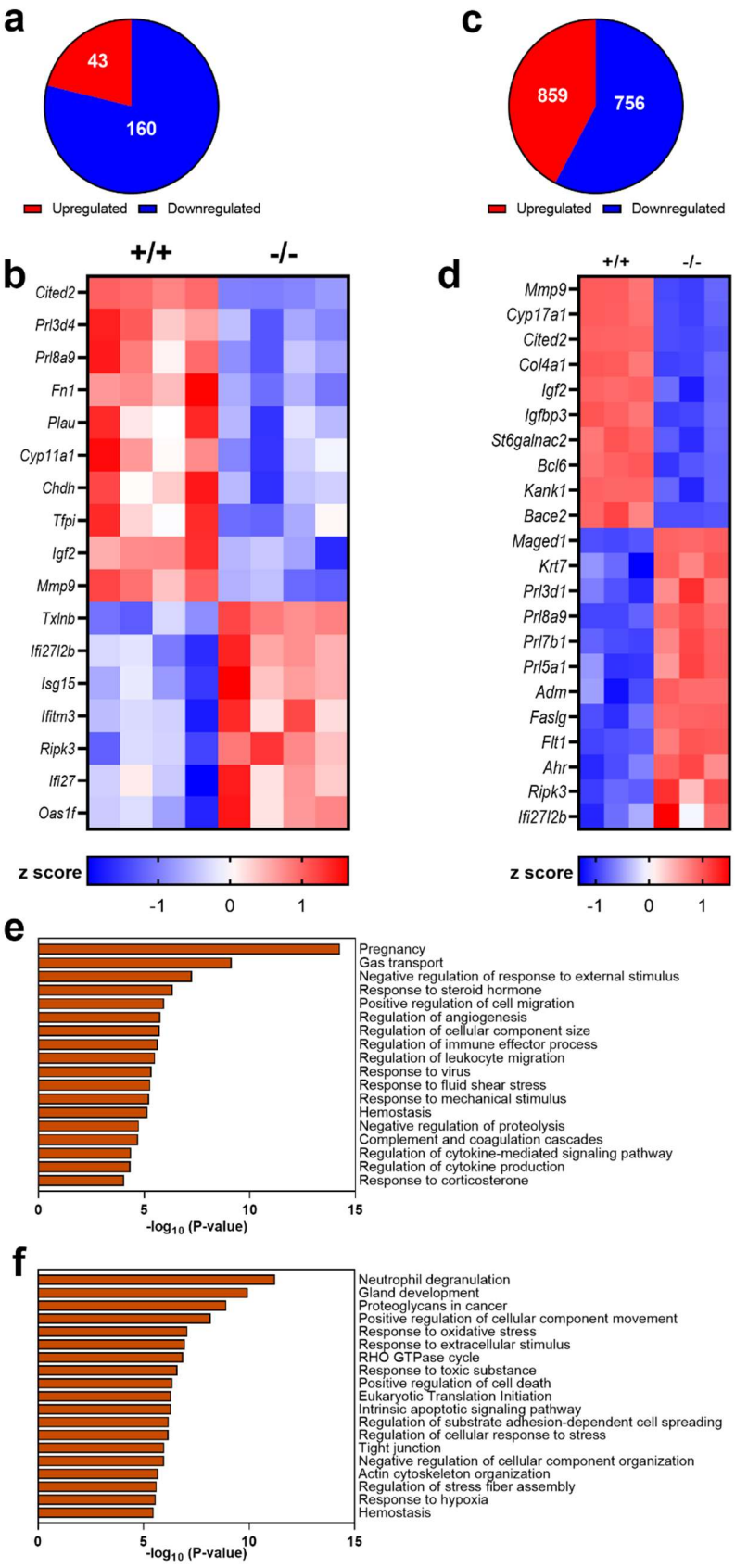

Fig. 4 CITED2 deficiency affects rat junctional zone and trophoblast cell transcriptomes. a. Significantly upregulated and downregulated transcripts from RNA-seq analysis of rat 14.5 junctional zone tissue from wild type (+/+) and *Cited2* null (-/-) rats, n=4, log_2-fold change in either direction>1.5, $p<0.05$. **b.** Heatmap showing select transcripts from RNA-seq analysis of wild type (+/+) and *Cited2* null (-/-) rat 14.5 junctional zone tissue. **c.** Significantly upregulated and downregulated transcripts from RNA-seq analysis of differentiated wild type (+/+) and *Cited2* null (-/-) rat trophoblast stem (**TS**) cells, n=3, log_2-fold change in either direction>1.5, $p<0.05$. **d.** Heatmap showing select transcripts from RNA-seq analysis of differentiated rat TS cells from RNA-seq analysis of wild type (+/+) and *Cited2* null (-/-) differentiated TS cells. **e.** Gene Ontology (**GO**) enriched terms for DEGs from wild type (+/+) versus *Cited2* null (-/-) rat 14.5 junctional zone RNA-seq analysis. **f.** GO enriched terms for DEGs from wild type (+/+) versus *Cited2* null (-/-) rat TS cell RNA-seq analysis.

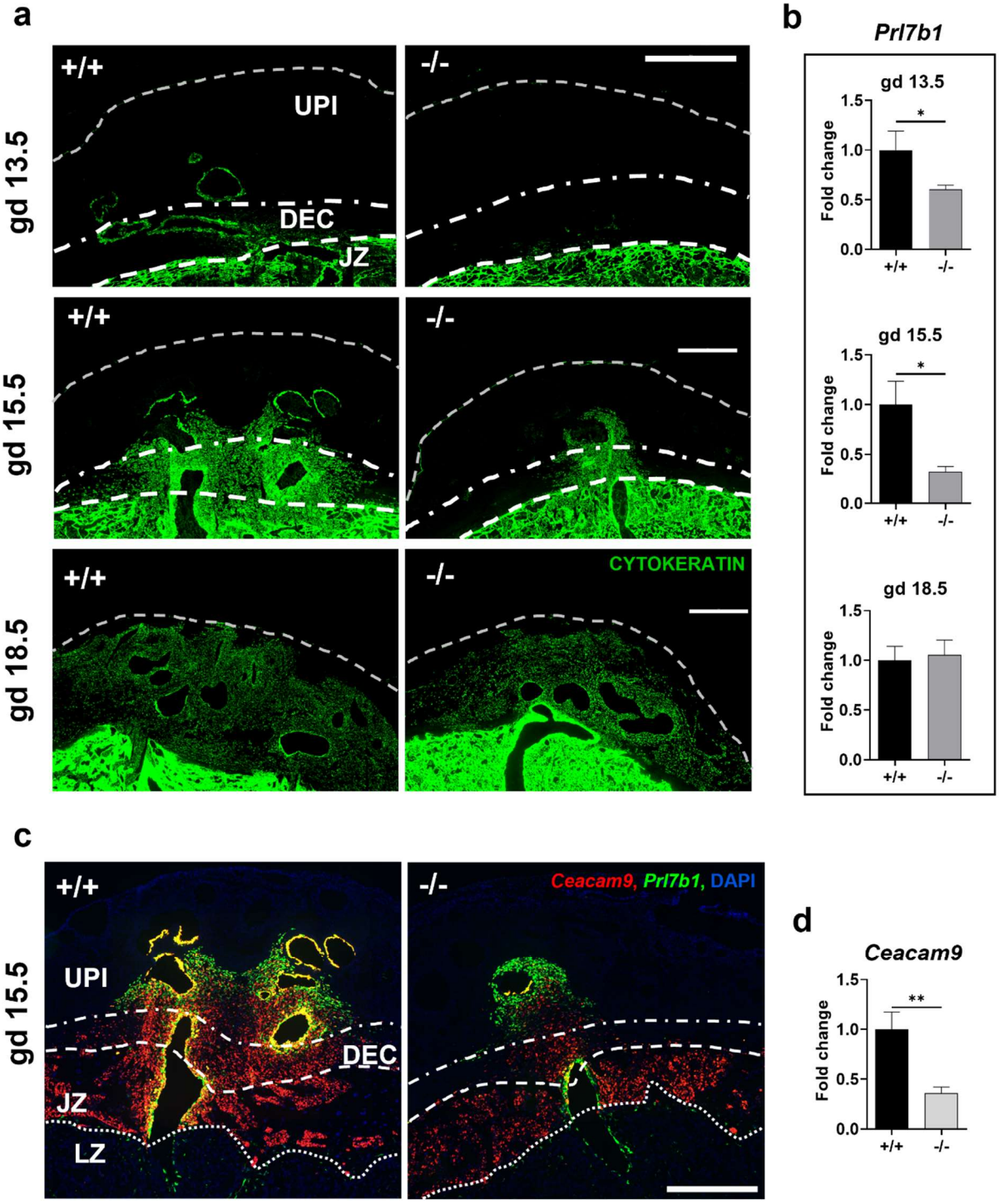

Fig. 5 Intrauterine trophoblast cell invasion is delayed in *Cited2* null rat placentation sites. **a.** Representative images of wild type (+/+) and *Cited2* null (-/-) rat gd 13.5, 15.5 and 18.5 placentation sites immunostained for cytokeratin (green). Scale bars=1000 µm. **b.** Relative expression of transcripts associated with invasive trophoblast (*Prl7b1*) from wild type (+/+) and *Cited2* null (-/-) gd 13.5 decidual tissue and uterine placental interface tissue at gd 15.5 and 18.5. Graphs depict mean values ± SEM, n=11-24, unpaired t-test, *p<0.05. **c.** *In situ* hybridization showing *Ceacam9* (red) and *Prl7b1* (invasive trophoblast marker, green) transcript localization

in gd 15.5 wild type (+/+) and *Cited2* null (-/-) rat placentation sites, scale bar=1000 µm. **d.** Relative expression of *Ceacam9* transcripts in gd 15.5 uterine placental interface tissue. Shown are mean values ± SEM, n=12-14, unpaired t-test, **p<0.01. Uterine placental interface (**UPI**), decidua (**DEC**), junctional zone (**JZ**), labyrinth zone (**LZ**).

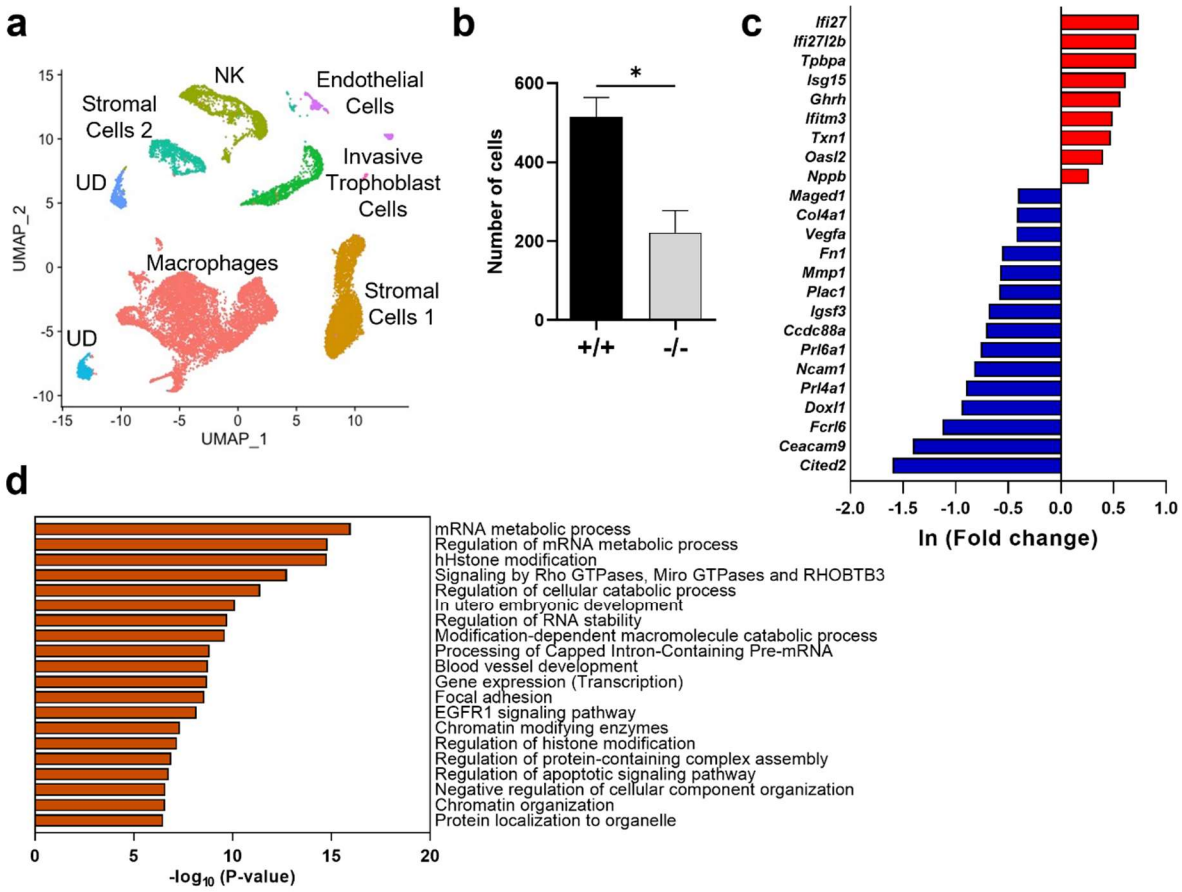

Fig. 6 CITED2 deficiency affects the rat invasive trophoblast cell phenotype. Single cell-RNA sequencing was performed on wild type (+/+) and *Cited2* null (-/-) gd 18.5 uterine-placental interface tissue samples. **a.** UMAP plot showing cell clustering in wild type (+/+) and *Cited2* null (-/-) gd 18.5 uterine-placental interface tissue. UD, unidentified cluster. **b.** Number of analyzed cells in the invasive trophoblast cell cluster. Graph represents mean values ± SEM, n=3, unpaired t-test, *p<0.05. **c.** Bar plot showing select DEGs in the invasive cell cluster (upregulated shown in red; downregulated shown in blue). **d.** Gene Ontology enriched terms for DEGs from the invasive trophoblast cell cluster.

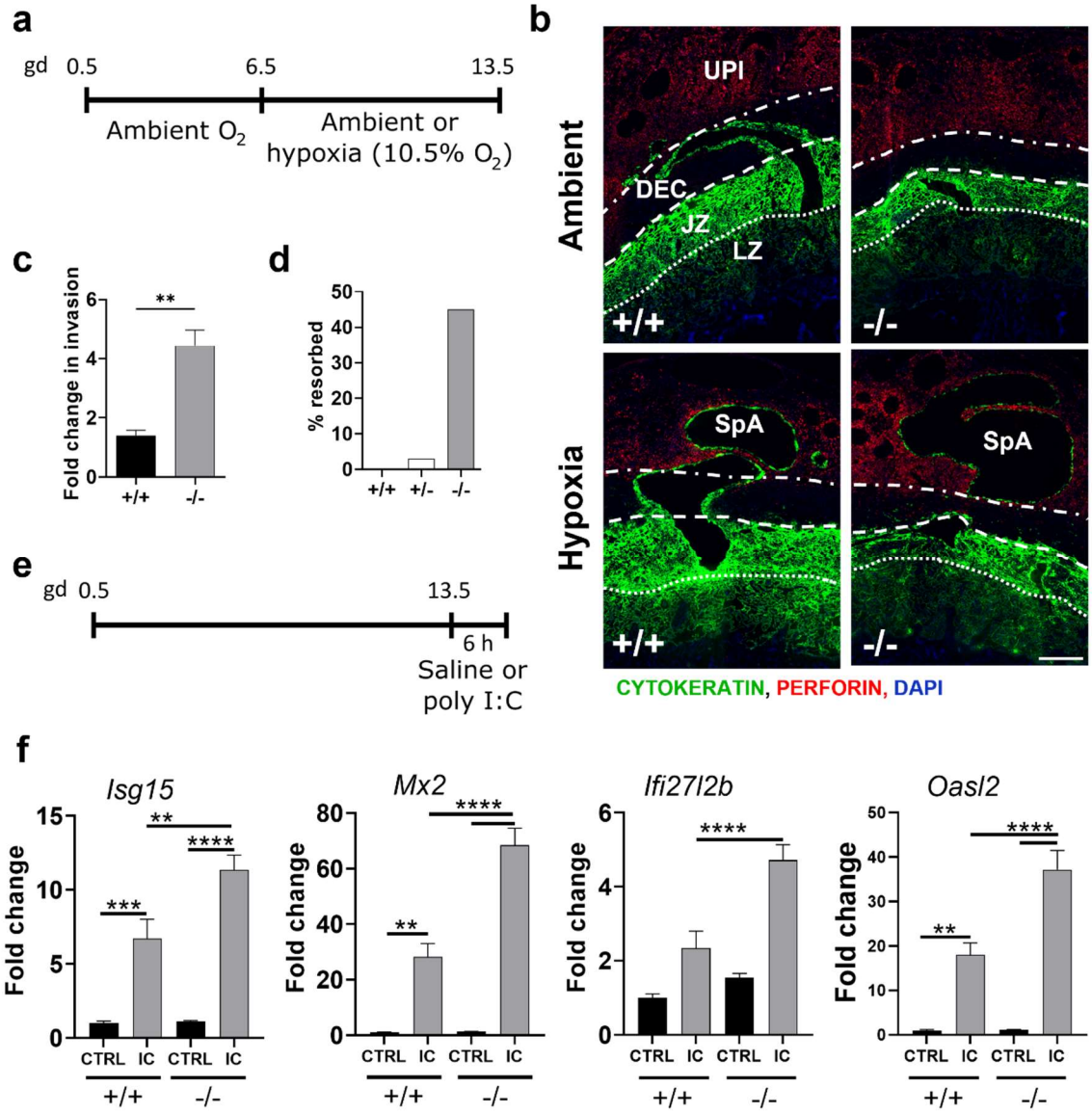

Fig. 7 CITED2 modulates rat placental responses to physiological stressors. a. Schematic of the experimental timeline for hypoxia exposure. **b.** Representative images of wild type (+/+) and *Cited2* null (-/-) rat gd 13.5 placentation sites exposed to ambient or hypoxic (10.5% oxygen) conditions. Sections were immunostained for cytokeratin (green), perforin (red), and DAPI (blue). Scale bar=500 µm. Uterine placental interface (**UPI**), Decidua (**DEC**), Junctional Zone (**JZ**), labyrinth zone (**LZ**), and Spiral artery (**SpA**). **c.** Depth of invasion was quantified, and fold changes calculated for hypoxic relative to ambient conditions, n=5-9. **d.** Resorption rate assessed on gd 18.5 for individual genotypes from *Cited2*$^{+/-}$ females bred to *Cited2*$^{+/-}$ males and exposed to ambient of hypoxic conditions, n=20-33. **e.** Schematic of the experimental timeline for polyinosinic:polycytidylic acid (**polyI:C**) treatment, **f.** Relative expression of *Isg15*, *Mx2*, *Ifi27I2b*, and *Oasl2* in junctional zone tissue from control (saline treated; **CTRL**) and polyI:C treated (**IC**) wild type (+/+) and *Cited2* null (-/-) animals.; n=8-17. Shown are mean values ± SEM, one-way analysis of variance, Tukey's post-hoc test. *p<0.05, **p <0.01, ***p <0.001. ****p <0.0001.

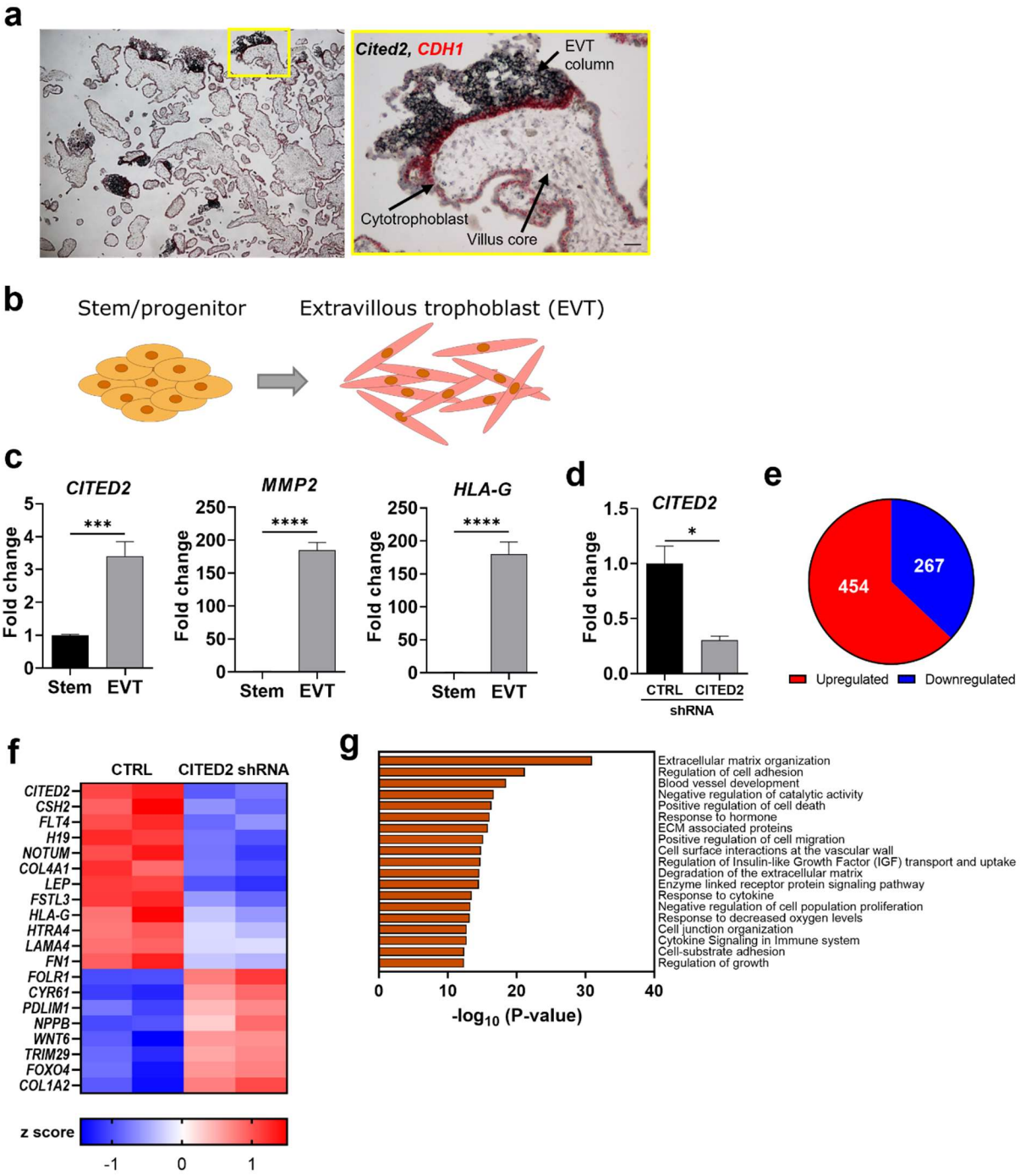

Fig. 8 CITED2 regulates human extravillous trophoblast (EVT) cell differentiation. a. *In situ* hybridization showing *CITED2* transcript localization in first trimester human placenta. C*ITED2* transcripts (black) were co-localized with E-cadherin (*CDH1*, red; marker of cytotrophoblast progenitor cells) transcripts. High magnification image of an EVT cell column and villus (yellow box) are shown in the right panel. The scale bar in the magnified image is 100 µm. **b.** Schematic showing human trophoblast stem (**TS**) cell differentiation from stem/progenitor state to EVT cells. **c.** Relative expression of *CITED2* and EVT cell signature transcripts (*MMP2* and *HLA-G*) in human TS cells in the stem state and following eight days of

EVT cell differentiation, n=5. **d.** Relative expression of *CITED2* transcript levels in EVT cells expressing control (**CTRL**) shRNA or CITED2 shRNA, n=3. Graphs represent mean values ± SEM, unpaired t-test, *p<0.05, ***p <0.001. ****p <0.0001. **e.** Significantly upregulated and downregulated transcripts from RNA-seq analysis of CTRL shRNA versus CITED2 shRNA samples, n=3, and $\log_2$-fold change (**FC**) in either direction>1.5, p<0.05. **f.** Heatmap showing select transcripts from RNA-seq analysis of CTRL shRNA versus CITED2 shRNA treated EVT cells. **g**. Gene Ontology enriched terms for DEGs from CTRL shRNA versus CITED2 shRNA treated EVT cells.